The KTS splice variant of WT1 is essential for ovarian determination in mice

Gregoire, E.P.; Cian, M.C. de; Migale, R.; Perea-Gomez, A.; Schaub, S.; Bellido-Carreras, N.; ... ; Chaboissier, M.C.

DEVELOPMENT

The –*KTS* splice variant of WT1 is essential for ovarian determination in mice

Elodie P. Gregoire[1], Marie-Cécile De Cian[1]†, Roberta Migale[2]†, Aitana Perea-Gomez[1], Sébastien Schaub[3], Natividad Bellido-Carreras[1], Isabelle Stévant[4,5], Chloé Mayère[4,5], Yasmine Neirijnck[1], Agnès Loubat[1], Paul Rivaud[6], Miriam Llorian Sopena[2], Simon Lachambre[7], Margot M. Linssen[8], Peter Hohenstein[8], Robin Lovell-Badge[2], Serge Nef[4,5], Frédéric Chalmel[6], Andreas Schedl[1], Marie-Christine Chaboissier[1]*

Sex determination in mammals depends on the differentiation of the supporting lineage of the gonads into Sertoli or pregranulosa cells that govern testis and ovary development, respectively. Although the Y-linked testis-determining gene *Sry* has been identified, the ovarian-determining factor remains unknown. In this study, we identified –KTS, a major, alternatively spliced isoform of the Wilms tumor suppressor WT1, as a key determinant of female sex determination. Loss of –*KTS* variants blocked gonadal differentiation in mice, whereas increased expression, as found in Frasier syndrome, induced precocious differentiation of ovaries independently of their genetic sex. In XY embryos, this antagonized *Sry* expression, resulting in male-to-female sex reversal. Our results identify –KTS as an ovarian-determining factor and demonstrate that its time of activation is critical in gonadal sex differentiation.

In mice, sex is genetically determined by the constitution of the sex chromosomes. This leads to testis or ovary development in XY and XX embryos, respectively, which, in turn, influences the sexual development of the whole individual. Before sex determination, WNT/β-catenin signaling mediated by R-spondin1 (RSPO1) contributes to the proliferation of the gonadal progenitors in both sexes (*1*). In XY gonads, at around embryonic day (E) 11.5, RSPO1/WNT/β-catenin is down-regulated and *Sry* and its direct target *Sox9* are up-regulated in a subset of progenitors derived from the overlying coelomic epithelium (*2*–*4*). These transcription factors induce Sertoli cell differentiation. Once differentiated, they no longer express *Sry* but express other genes, including *Amh* (*5*–*7*), and establish the fate of the testis. In XX gonads, pregranulosa cell differentiation occurs slightly later, around E12.0 to 12.5, as shown by their loss of bipotentiality (*8*–*10*), the de novo expression of the transcription factor FOXL2 (*11*), and the stabilization of RSPO1/WNT/β-catenin signaling (*12*, *13*). However, the gene(s) initiating ovarian differentiation have remained unknown (*14*).

One of the key factors in the early development of the gonad is the Wilms tumor suppressor WT1, a zinc-finger transcriptional regulator (*15*). *WT1* (human)/*Wt1* (mouse) encodes two major alternative spliced isoforms that do or do not include the three amino acids KTS (lysine, threonine, and serine) between the two last zinc fingers. These isoforms are named +KTS and –KTS, respectively. Whereas –KTS acts as a transcriptional activator or repressor depending on the cellular context, the insertion of +KTS abrogates DNA binding and promotes the subnuclear localization of WT1 in nuclear speckles (*16*, *17*). A simple imbalance of the ratio of both isoforms in favor of –*KTS* is the molecular basis of Frasier syndrome, characterized by male-to-female sex reversal (*18*, *19*) associated with the down-regulation of *Sry* as evidenced in the mouse model (*20*).

Results

Distribution of –KTS transcripts during gonadal development

To determine the distribution of WT1 splice variants in E11.5 XY mouse gonads, we carried out BaseScope in situ hybridizations. Scoring revealed cellular heterogeneity, with cells containing variable amounts of +*KTS* or –*KTS* transcripts (Fig. 1A and fig. S1A). This observation was confirmed with single-cell RNA sequencing (scRNA-seq) analysis of the splice junction reads obtained from sorted cells dissected from E11.5 mouse gonads (Fig. 1B). Next, we examined single-cell transcriptomic data of the supporting cell lineage in both sexes from E10.5 to E13.5 (*8*) (Fig. 1C and fig. S1B). Although +*KTS* exhibited similar mRNA levels between XY and XX gonads at E10.5 and E[illegible] –*KTS* transcripts were detected in greater amounts in XY gonads at E11.5 before increasing in XX gonads at E12.5, time points that coincide respectively with Sertoli and pregranulosa cell differentiation.

–KTS is required for the differentiation of the supporting cells

To address the contribution of –*KTS* to sex determination, we revisited the mouse model of –*KTS* ablation (–*KTS*$^{-}$/–*KTS*$^{-}$ is denoted as –*KTS KO*) that results in gonadal dysgenesis (*20*) (fig. S2, A and B). We performed single-cell transcriptome profiling of wild-type and mutant gonadal cells collected at around E12.0 (Fig. 1, D to I, and table S1). Cells were projected in a two-dimensional (2D) space by using uniform manifold approximation and projection (UMAP) and partitioned into 39 clusters (Fig. 1D). Cluster annotation identified Sertoli and pregranulosa cells in the controls determined from the expression of known markers (Fig. 1, E to G, and fig. S3, A and B); however, these clusters were not present in –*KTS KO* gonads (Fig. 1, E to H, and fig. S3B). Nevertheless, presupporting cells were observed in –*KTS* mutants of both sexes, as revealed by the expression of *Runx1* (mRNA)/RUNX1 (protein) at E12.0 [fig. S3B, cluster 3 (c3)] and at E12.5 (Fig. 2A and fig. S4). XY –*KTS*-deficient gonads exhibited a few scattered cells expressing SOX9, contrasting with the widespread SOX9-positive Sertoli cells that formed nascent testis cords in XY controls (Fig. 2B). Furthermore, XY –*KTS*-deficient gonads were devoid of *Amh*/AMH expression (Fig. 2, C and D, and fig. S5, A and B) and instead abnormally maintained *Rspo1* and SRY at E12.5 and until birth (fig. S2, C and E, and fig. S5, C and E). Together, our results indicate that the presupporting cells did not differentiate as bona fide Sertoli cells in the absence of –KTS. Despite the significantly reduced expression of *Sox9* (P value = 0.0035), the XY –*KTS KO* presupporting cells failed to differentiate into pregranulosa cells, as demonstrated by the almost complete absence of *Foxl2*/FOXL2 expression at E12.5 (Fig. 2, B and D, and fig. S3). Similarly, *Foxl2*/FOXL2 expression was strongly reduced in XX –*KTS KO* gonads, further supporting the importance of –KTS for the differentiation of the pregranulosa lineage and the activation of the female program (Fig. 2, B and D, and fig. S3). At around birth, the expression of *Sox9*/SOX9 and *Foxl2*/FOXL2 remained low in –*KTS*-deficient gonads of both sexes, and SOX9/FOXL2 double-positive cells were detected (fig. S5, F to H), indicating poor differentiation of the supporting lineage. Together, these data demonstrate that –*KTS* is dispensable for the specification of presupporting cells but is necessary to stabilize Sertoli cell differentiation and essential to initiate pregranulosa cell differentiation.

[1]Université Côte d'Azur, INSERM, CNRS, Institut de Biologie Valrose (iBV), 06108 Nice, France. [2]The Francis Crick Institute, London NW1 1AT, UK. [3]Sorbonne Université, CNRS, Development Biology Laboratory (LBDV), 06234 Villefranche sur Mer, France. [4]Department of Genetic Medicine and Development, University of Geneva, 1211 Geneva, Switzerland. [5]iGE3, Institute of Genetics and Genomics of Geneva, University of Geneva, 1211 Geneva, Switzerland. [6]Univ Rennes, INSERM, EHESP, IRSET (Institut de Recherche en Santé, Environnement et Travail)-UMR_S 1085, 35000 Rennes, France. [7]Infinity, INSERM, CNRS, University Toulouse III, 31024 Toulouse, France. [8]Central Animal and Transgenic Facility and Department of Human Genetics, Leiden University Medical Center, 2333ZA Leiden, Netherlands.
***Corresponding author. Email: marie-christine.chaboissier@univ-cotedazur.fr**
†These authors contributed equally to this work.

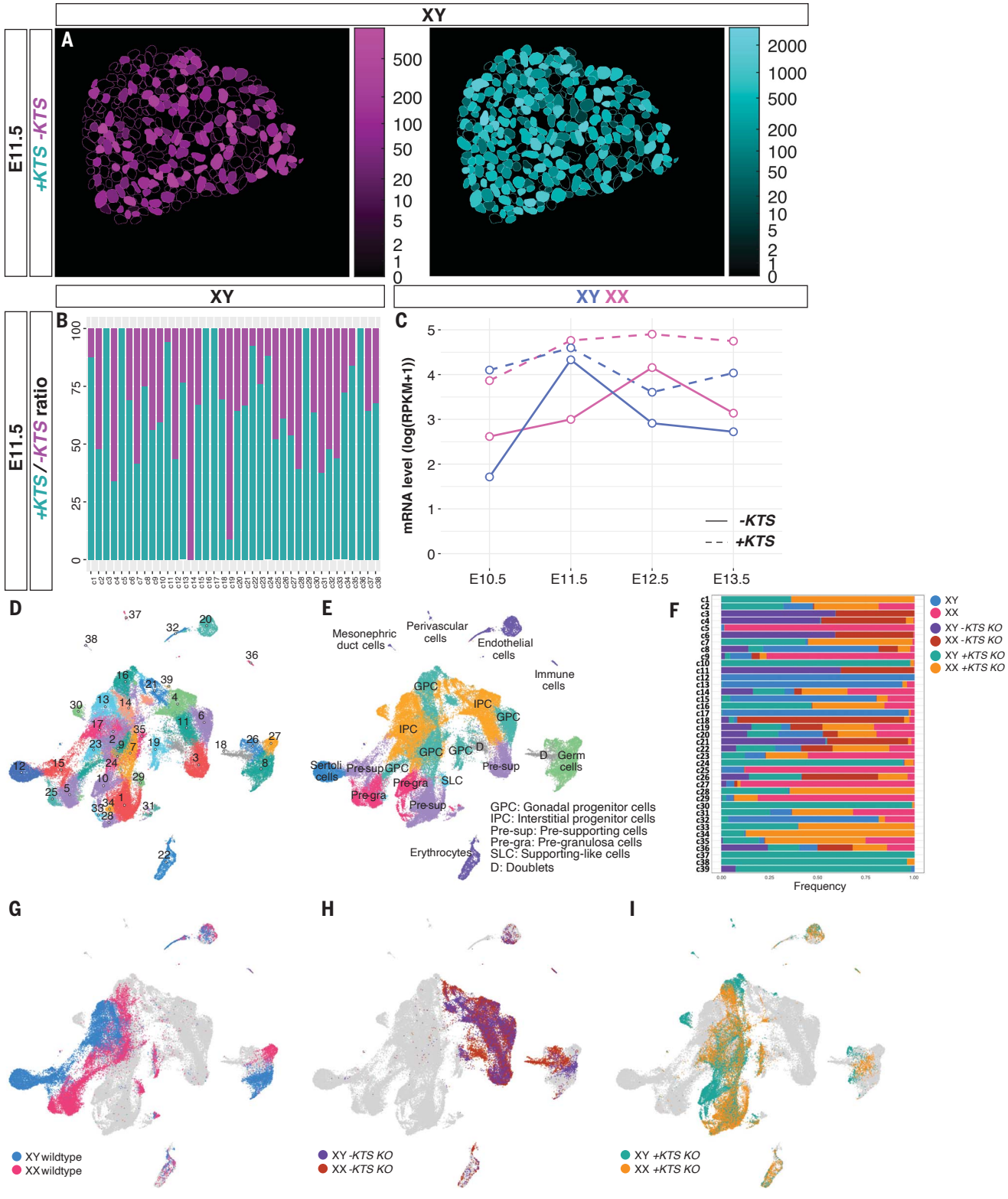

Fig. 1. Dynamic distribution of +KTS and −KTS transcripts and single-cell transcriptomic analysis of −KTS KO and +KTS KO during early mouse-gonad development. (**A**) Representative area distribution of *−KTS* (magenta) and *+KTS* (cyan) transcripts from Basescope in situ hybridizations on XY gonad sections at E11.5 [21 tail somites (ts)] in square micrometers per nucleus measured with DicHysto protocol. Data from both gonads are representative of biological and technical duplicates. (**B**) *−KTS* and *+KTS* mRNA ratio in E11.5 (21 ts) XY wild-type individual cells. (**C**) *+KTS* and *−KTS* transcript levels in single-cell transcriptomic dataset of differentiating supporting cells. RPKM, reads per kilobase million. (**D**) UMAP projection of the 75,360 cells colored by clusters or (**E**) by associated cell types. (**F**) Association of cell clusters with genotypes. (**G** to **I**) UMAP projection by genotypes with (G) XY (blue) and XX wild type (pink); (H) XY (purple) and XX *−KTS KO* (*−KTS*$^{-}$/*−KTS*$^{-}$) (brown); and (I) XY (green) and XX *+KTS KO* (*+KTS*$^{-}$/*+KTS*$^{-}$) gonads (orange).

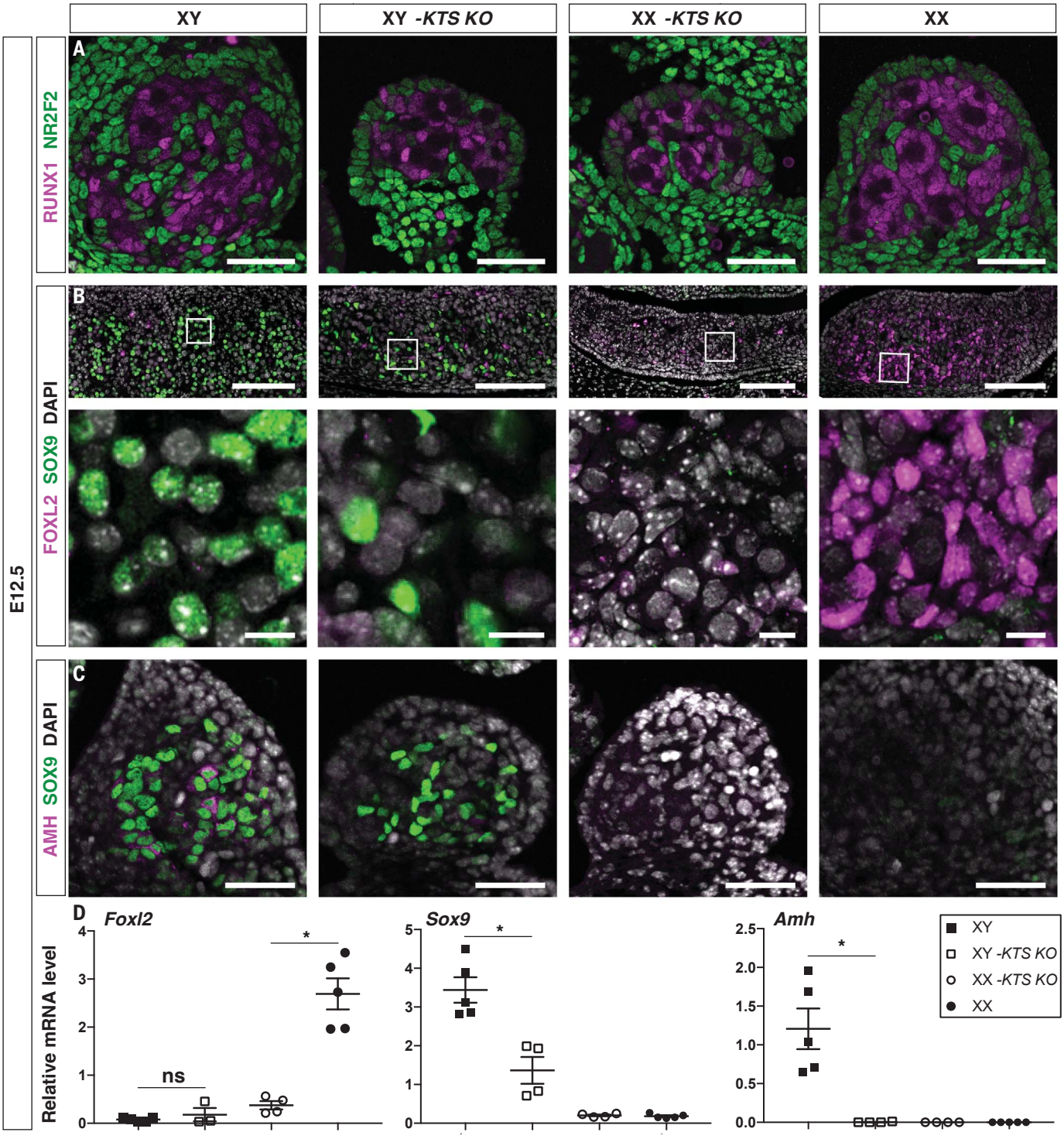

Fig. 2. −KTS is necessary for sex differentiation of the supporting cells. Immunodetection of (**A**) the presupporting cell marker RUNX1 (magenta) and the progenitor marker NR2F2 (green) at E12.5 (scale bars, 50 μm), (**B**) the Sertoli cell marker SOX9 (green) and pregranulosa cell marker FOXL2 (magenta) (scale bars, 100 μm and 10 μm, respectively), and (**C**) SOX9 (green) and AMH (magenta) (scale bars, 50 μm) in the indicated genotypes. Data for (A) to (C) are representative of triplicate biological replicates. Nuclei labeled with 4′,6-diamidino-2-phenylindole (DAPI) are shown in white. (**D**) Quantification of *Foxl2*, *Sox9*, and *Amh* transcripts after normalization to *Gapdh* by RT-qPCR. Data are shown as means ± SEM. *−KTS KO* denotes $-KTS^{-}/-KTS^{-}$.

Absence of +KTS *triggers an increase of* −KTS *amounts*

In patients with Frasier syndrome, heterozygous mutations in WT1 prevent the production of *+KTS,* resulting in higher amounts of *−KTS* variants (*18*, *19*). Given the role of *−KTS* in ovarian determination, we investigated the contribution of this increase to sex reversal in the *+KTS KO* ($+KTS^{-}/+KTS^{-}$) mouse model (*20*). At E12.5, XY *+KTS* mutant gonads were enriched for RUNX1- and FOXL2-positive pregranulosa cells and contained rare Sertoli cells, as expected for male-to-female sex reversal (Fig. 3A and fig. S6A). Next, we verified that *−KTS* transcripts were twice as abundant in

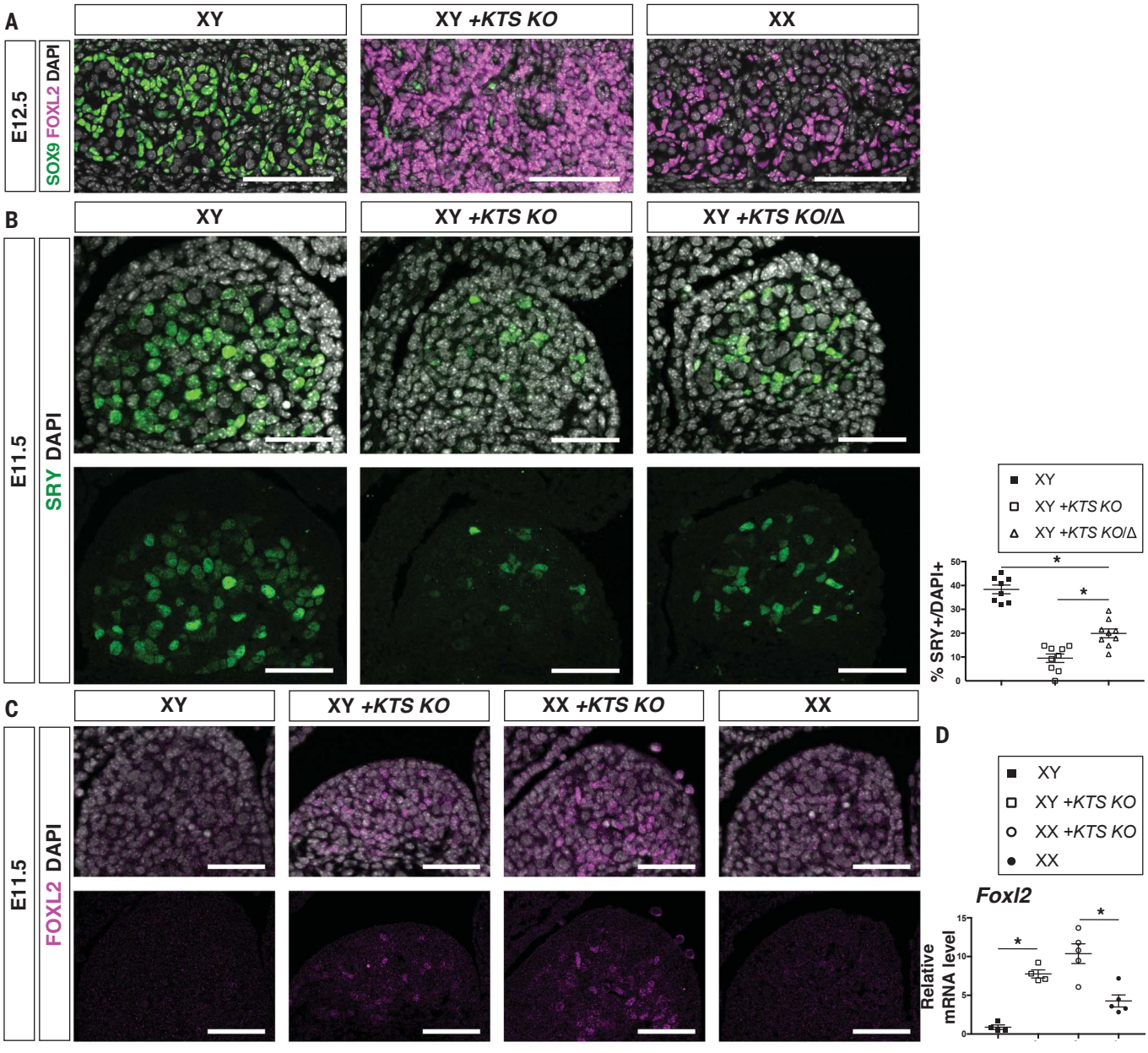

Fig. 3. Early pregranulosa cell differentiation occurs in XY and XX *+KTS KO* gonads. (**A**) Immunofluorescence of the Sertoli cell marker SOX9 (green) and the pregranulosa cell marker FOXL2 (magenta) in indicated genotypes at E12.5 (n = 4 embryos). Scale bars, 100 μm. (**B**) Immunostaining of SRY (green) at E11.5 (21 ± 1 ts) in XY, XY *+KTS KO* (*+KTS*$^{-}$/*+KTS*$^{-}$), and XY compound heterozygotes (*+KTS KO*/Δ denotes *+KTS*$^{-}$/*Wt1*$^{-}$). Scale bars, 50 μm. Quantification of SRY+ cells normalized to DAPI+ cells labeled in white in the upper panel. n = 4 embryos, two sections per embryo. Data are shown as means ± SEM. (**C**) Immunodetection of the pregranulosa cell marker FOXL2 in indicated genotypes of triplicate biological replicates at 20 to 21 ts. Scale bars, 50 μm. (**D**) Relative mRNA expression of *Foxl2* normalized to *Gapdh* at 20 to 21 ts. Data are shown as means ± SEM.

+KTS KO gonads as in controls (fig. S6B). In addition, total WT1 protein levels were similar in XY *+KTS KO* and control gonads, confirming that absence of +KTS is compensated with an increase of −KTS isoforms (fig. S6C).

Precocious pregranulosa cell differentiation prevents Sry activation in the mouse Frasier model

Sex reversal in *+KTS KO* embryos is caused by a failure of *Sry* activation (*20*, *21*). To determine if this arises from the lack of *+KTS* or from an increase in *−KTS* variants, we compared the number of SRY-positive cells in *+KTS KO* and *+KTS KO*/Δ compound embryos, both of which lack alleles encoding *+KTS* and contain two and one allele encoding *−KTS,* respectively. The number of SRY-expressing cells was higher in *+KTS KO*/Δ than in XY *+KTS KO* gonads, indicating that *Sry* expression does not require +KTS but is antagonized by the higher level of −KTS (Fig. 3B). Furthermore, *Rspo1* was abundant in XY *+KTS KO* gonads at E11.5, a stage when it is down-regulated in XY gonads, and *Foxl2*/FOXL2 expression was markedly elevated in XY and XX *+KTS KO* gonads (Fig. 3, C and D, and fig. S6E). This suggests precocious pregranulosa cell differentiation irrespective of the genetic sex.

−KTS is sufficient to induce ovarian development

Single-cell transcriptome profiling of XY and XX *+KTS KO* gonads at E12.0 (Fig. 1, D to F,

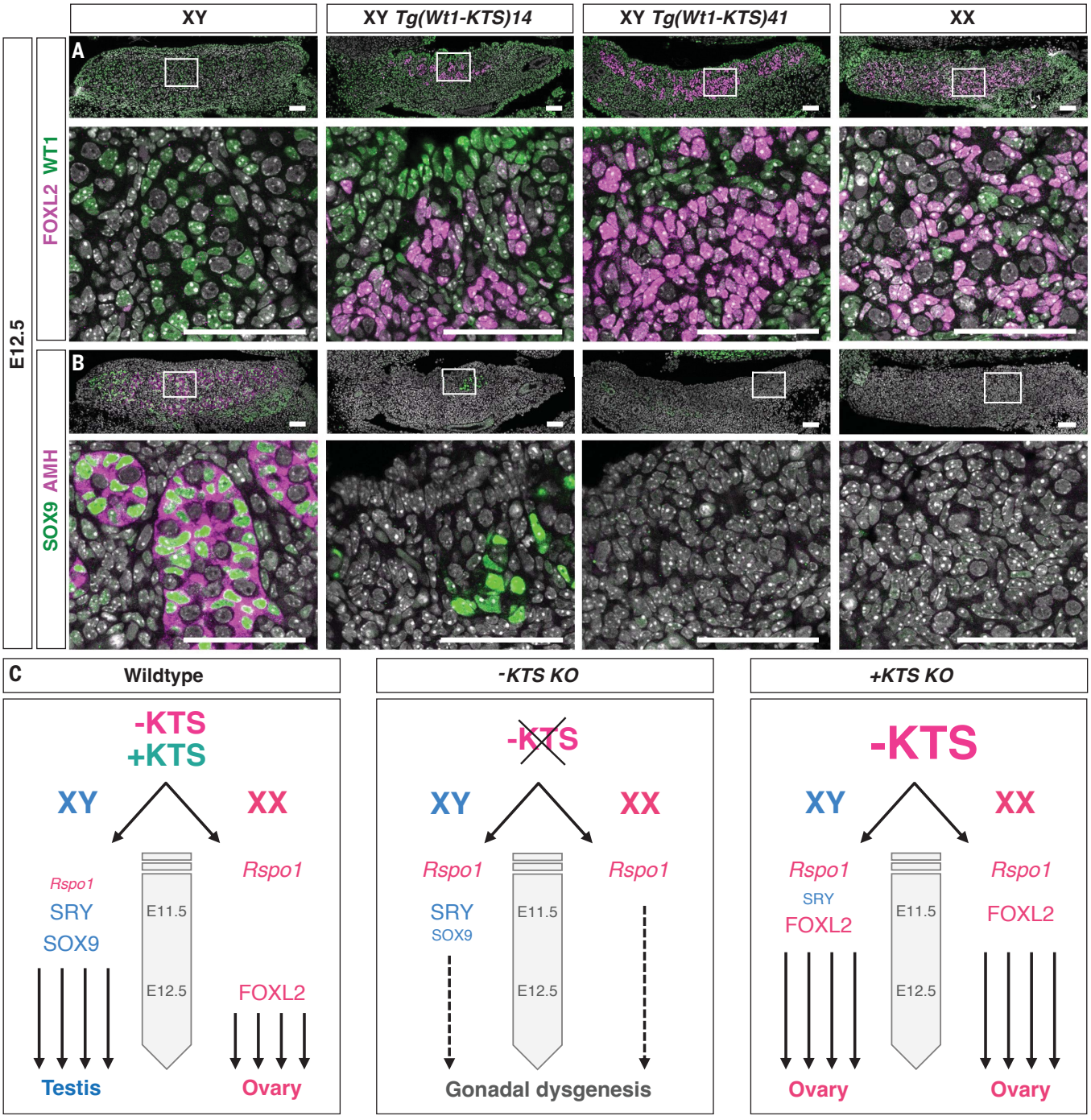

Fig. 4. –KTS induces pregranulosa cell differentiation in XY transgenic gonads. (**A**) Immunofluorescence of the pregranulosa cell marker FOXL2 (magenta) and WT1 (green) in the indicated genotypes at E12.5. Scale bars, 50 μm. (**B**) Immunostaining of the Sertoli cell markers SOX9 (green) and AMH (magenta) in indicated genotypes. Scale bars, 50 μm. (**C**) Model of supporting cell differentiation in wild-type and *KTS* mutant gonads: Absence of *–KTS* in *–KTS KO* gonads promotes the maintenance of *Rspo1* transcripts and impairs SOX9 and FOXL2 expression, leading to gonadal dysgenesis. Increasing –KTS in *+KTS KO* gonads results in ovarian differentiation in both genetic sexes.

and I, and fig. S3B) identified two pregranulosa cell clusters (c10 and c33) distinct from those found in XX controls (c5 and c25) and from XY Sertoli cells (c12). Further comparison of transcriptomes of these clusters confirmed that E12.0 *+KTS KO* cells are transcriptionally related to pregranulosa cells (fig. S7). Next, we used comparative analysis to identify genes that are activated or repressed by –KTS in the context of female sex determination (fig. S8). In XX *–KTS KO* presupporting cells, the expression of 319 genes was significantly deregulated [false discovery rate (FDR)–adjusted *P* value ≤ 0.05, data S4]. *Pdgfa* and *Tcf21,* reported to be targets of WT1 in other organs (*22*, *23*), were down-regulated, whereas *Igf2*—a direct target of WT1 (*24*)—and genes highly expressed in bipotent presupporting cells including *Sprr2d* (*25*), *Wnt6* (*26*), and *Nr0b1* (*27*), were up-regulated in XX *–KTS KO* presupporting cells and down-regulated in XX *+KTS KO*

pregranulosa cells, suggesting that they are repressed by –KTS during sex determination. Altogether, our data suggested that increased –KTS, rather than loss of +KTS, was responsible for XY sex reversal in the *+KTS KO* model. To test whether –KTS was sufficient to induce ovarian differentiation in a XY wild-type gonad, we performed transient additive transgenesis using a bacterial artificial chromosome (BAC) construct covering the *Wt1* locus, in which we introduced the classical Frasier mutation in intron 9 (interference with +KTS production). Three out of four XY transgenic animals showed the presence of FOXL2-positive cells, indicating that –KTS promotes differentiation of pregranulosa cells in XY gonads (Fig. 4, A and B, and fig. S9, A and B). Moreover, reverse transcription quantitative polymerase chain reaction (RT-qPCR) analysis of genotypes producing different levels of –KTS suggested that *–KTS* must reach a threshold to robustly activate *Foxl2* expression (fig. S9C).

We can conclude that the altered expression of *+KTS* caused by mutations in the donor splice site in intron 9 of *Wt1* promotes an increase of the amount of –KTS, which, in turn, prematurely activates ovarian differentiation, prevents *Sry* up-regulation, and impairs testis development (Fig. 4C). –KTS thus represents a key actor in gonad development that is required to initiate ovarian development.

Discussion

Here, we provide evidence that sex determination depends not only on the up-regulation of the sex-determining factors *Sry* and *–KTS* for male and female fates, respectively, but also on their timing (*28*–*30*). This is an important concept because *–KTS* is an autosomal factor expressed in both XY and XX gonads. In wild-type mice, *Sry* acts before *–KTS*, thus securing testis development in XY gonads. If *Sry* expression is impaired or delayed, or if *–KTS* is up-regulated prematurely, such as in the Frasier syndrome model (*+KTS KO*), the pregranulosa cell differentiation is accelerated, resulting in male-to-female sex reversal. After the peak of SRY action (*30*), –KTS becomes necessary to maintain Sertoli cell differentiation in XY embryos and to initiate pregranulosa cell differentiation in XX embryos (Fig. 4C). Although differences in timing and dynamics of sex determination make a direct comparison between mouse and human data difficult, the sex-reversal phenotype in mice carrying intron 9 mutations suggests that this is a good mouse model for the human Frasier syndrome. Our data thus indicate that increased expression of –KTS, rather than loss (or reduction) of +KTS, is the primary cause of sex reversal in Frasier syndrome. Notably, a change of *+KTS*/*–KTS* ratio in favor of *–KTS* operates when the eggs of *Chelydra serpentina,* a turtle with temperature-dependent sex determination, are shifted from a male- to a female-producing temperature (*31*). This outcome suggests that the –KTS isoform of WT1 is also involved in ovarian determination outside of the mammalian class.

REFERENCES AND NOTES

1. A.-A. Chassot *et al*., *Development* **139**, 4461–4472 (2012).
2. R. Sekido, I. Bar, V. Narváez, G. Penny, R. Lovell-Badge, *Dev. Biol.* **274**, 271–279 (2004).
3. N. Gonen *et al*., *Science* **360**, 1469–1473 (2018).
4. J. Karl, B. Capel, *Dev. Biol.* **203**, 323–333 (1998).
5. M.-C. Chaboissier *et al*., *Development* **131**, 1891–1901 (2004).
6. P. De Santa Barbara *et al*., *Mol. Cell. Biol.* **18**, 6653–6665 (1998).
7. M. Bullejos, P. Koopman, *Dev. Dyn.* **221**, 201–205 (2001).
8. I. Stévant *et al*., *Cell Rep.* **26**, 3272–3283.e3 (2019).
9. K. Harikae *et al*., *J. Cell Sci.* **126**, 2834–2844 (2013).
10. W. Niu, A. C. Spradling, *Proc. Natl. Acad. Sci. U.S.A.* **117**, 20015–20026 (2020).
11. D. Schmidt *et al*., *Development* **131**, 933–942 (2004).
12. P. Parma *et al*., *Nat. Genet.* **38**, 1304–1309 (2006).
13. D. M. Maatouk, L. Mork, A.-A. Chassot, M.-C. Chaboissier, B. Capel, *Dev. Biol.* **383**, 295–306 (2013).
14. M. Elzaiat, A.-L. Todeschini, S. Caburet, R. A. Veitia, *Clin. Genet.* **91**, 173–182 (2017).
15. J. A. Kreidberg *et al*., *Cell* **74**, 679–691 (1993).
16. C. Englert *et al*., *Proc. Natl. Acad. Sci. U.S.A.* **92**, 11960–11964 (1995).
17. S. H. Larsson *et al*., *Cell* **81**, 391–401 (1995).
18. S. Barbaux *et al*., *Nat. Genet.* **17**, 467–470 (1997).
19. B. Klamt *et al*., *Hum. Mol. Genet.* **7**, 709–714 (1998).
20. A. Hammes *et al*., *Cell* **106**, 319–329 (2001).
21. S. T. Bradford *et al*., *Hum. Mol. Genet.* **18**, 3429–3438 (2009).
22. Z. Y. Wang, S. L. Madden, T. F. Deuel, F. J. Rauscher 3rd, *J. Biol. Chem.* **267**, 21999–22002 (1992).
23. R. Bandiera *et al*., *Dev. Cell* **27**, 5–18 (2013).
24. A. Ward *et al*., *Gene* **167**, 239–243 (1995).
25. G. J. Bouma, Q. J. Hudson, L. L. Washburn, E. M. Eicher, *Biol. Reprod.* **82**, 380–389 (2010).
26. A. T. Cory, A. Boyer, N. Pilon, J. G. Lussier, D. W. Silversides, *Mol. Reprod. Dev.* **74**, 1491–1504 (2007).
27. A. Swain, E. Zanaria, A. Hacker, R. Lovell-Badge, G. Camerino, *Nat. Genet.* **12**, 404–409 (1996).
28. E. M. Eicher, L. L. Washburn, *J. Exp. Zool.* **228**, 297–304 (1983).
29. M. Bullejos, P. Koopman, *Dev. Biol.* **278**, 473–481 (2005).
30. R. Hiramatsu *et al*., *Development* **136**, 129–138 (2009).
31. T. Rhen, R. Fagerlie, A. Schroeder, D. A. Crossley 2nd, J. W. Lang, *Differentiation* **89**, 31–41 (2015).
32. S. Schaub, SebastienSchaub/DICHisto: Gregoire_et_al2023, Zenodo (2023); https://doi.org/10.5281/ZENODO.8329139.
33. S. Lachambre, Nuclei count in gonad, Version 3, Zenodo (2023); https://doi.org/10.5281/ZENODO.8345079.
34. S. Lachambre, Intensity measurement in gonad, Version 2, Zenodo (2023); https://doi.org/10.5281/ZENODO.8345091.

ACKNOWLEDGMENTS

We thank M. Cerciat for her help in the preparation of 10X Genomics libraries. Sequencing was performed by the GenomEast platform, a member of the France Génomique consortium (ANR-10-INBS-0009). We are grateful to F. Jian Motamedi for her advice on transgenesis. The microscopy was performed at the MICA facility, at the iBV (Institut de Biologie Valrose, Université Côte d'Azur, CNRS, INSERM, iBV, France). We acknowledge help from members of the PRISM Imaging Platform, from the Animal house at Ibv, and from C. Passot and M. Cutajar-Bossert for the management of funding. We are grateful to the FLOW, BABS, ASF, and BRF facilities of the Francis Crick Institute. We are also grateful to members of the A.S. and M.-C.C. groups for helpful discussions. **Funding:** This research was supported by Agence Nationale de la Recherche grant ANR-19-CE14-0022 SexDiff (M.-C.C.), Fondation Maladies Rares grant FONDATION-GenOmics 2018-1 181003 RNAseq (M.-C.C.), Agence Nationale de la Recherche grant ANR-20-CE14-0022 Ardigerm (M.-C.C.), and Swiss National Science Foundation grants 31003A_173070 (S.N.) and 310030_200316 (S.N.). The Francis Crick Institute receives its core funding from Cancer Research UK (FC001107), the UK Medical Research Council (FC001107), Wellcome (FC001107), and the UK Medical Research Council (U117512772) (R.M., M.L.S., and R.L.-B.). **Author contributions:** E.P.G., R.L.-B., A.S., and M.-C.C. contributed to the conception and design of the study. E.P.G., M.-C.D.C., R.M., A.P.-G., N.B.-C., and A.L. carried out mouse work, in situ hybridization (ISH), immunofluorescence, microscopy, scRNA-seq, and other experimental analysis. S.S. and S.L. performed image posttreatments for quantitative analysis of Basescope ISH and immunostainings. I.S., Y.N., C.M., P.R., M.L.S., and F.C. performed the bioinformatics analysis. E.P.G., M.M.L., P.H., and A.S. generated transgenesis. E.P.G., A.S., and M.-C.C. wrote the first draft of the manuscript. All authors contributed to manuscript revision and read and approved the submitted version. Funding and resources: S.N., R.L.-B., and M.-C.C. Supervision: M.-C.C. **Competing interests:** The authors declare that they have no competing interests. **Data and materials availability:** All data are available in the manuscript or the supplementary materials. The scRNA-seq datasets are available at the National Center for Biotechnology (NCBI) Gene Expression Omnibus (GEO): GSE207097, and in articles cited in the paper. Programs developed are available at Zenodo (*32*–*34*). **License information:** Copyright © 2023 the authors, some rights reserved; exclusive licensee American Association for the Advancement of Science. No claim to original US government works. https://www.science.org/about/science-licenses-journal-article-reuse. This research was funded in whole or in part by the Swiss National Science Foundation (grants 31003A_173070 and 310030_200316), a cOAlition S organization. The author will make the Author Accepted Manuscript (AAM) version available under a CC BY public copyright license.

SUPPLEMENTARY MATERIALS

science.org/doi/10.1126/science.add8831
Materials and Methods
Figs. S1 to S9
Tables S1 to S3
References (*35*–*49*)
Data S1 to S4
MDAR Reproducibility Checklist

Submitted 13 July 2022; resubmitted 3 August 2023
Accepted 29 September 2023
10.1126/science.add8831